Transverse Viscous Transport in Classical Solid States

Akira Furukawa[*]
Institute of Industrial Science, University of Tokyo, Meguro-ku, Tokyo 153-8505, Japan

(Received 8 October 2019; revised 25 August 2021; accepted 18 October 2021; published 6 December 2021)

The transverse velocity time correlation function $\tilde{C}_T(k,\omega)$ with k and ω being the wave number and the frequency, respectively, is a fundamental quantity in determining the transverse mechanical and transport properties of materials. In ordinary liquids, a nonzero value of $\tilde{C}_T(k,0)$ is inevitably linked to viscous material flows. Even in solids where significant material flows are precluded due to almost frozen positional degrees of freedom, our molecular dynamics simulations reveal that $\tilde{C}_T(k,0)$ takes a nonzero value, whereby the time integration of the velocity field shows definite diffusive behavior with diffusivity $\tilde{C}_T(k,0)/3$. This behavior is attributed to viscous transport accompanying a small random convection of the velocity field (the *inertia* effect), and the resultant viscosity is measurable in the Eulerian description: the constituent particles that substantially carry momenta fluctuate slightly around their reference positions. In the Eulerian description, the velocity field is explicitly associated with such fluctuating instantaneous particle positions, whereas in the Lagrangian description, this is not the case. The present study poses a fundamental problem for continuum mechanics: reconciling liquid and solid descriptions in the limit of the infinite structural relaxation time.

DOI: 10.1103/PhysRevLett.127.245901

Viscosity is one of the most fundamental transport properties of liquids [1]. In elastic solids, although the importance of viscosity has frequently been considered [2], we still do not fully understand its role and mechanism. In solids, as with liquids, the velocity (momentum) fields are generally regarded as “gross variables,” for which dissipation channels are expected as opposed to the energy injection due to thermal fluctuations. In particular, for the transverse velocity field, the only possible dissipation channel is expected to be the shear viscosity.

A clue to this problem can be obtained by examining the velocity time correlation function (VTCF): according to the generalized hydrodynamics [3–5], the transverse VTCF in the wave number (k) and frequency (ω) space, $\tilde{C}_T(k,\omega)$, is related to the k-dependent shear viscosity $\eta(k)$ as

$$\lim_{\omega\to 0}\tilde{C}_T(k,\omega) \cong \frac{2T}{k^2\eta(k)}, \qquad (1)$$

where T is the temperature measured in units of Boltzmann’s constant. For details of this relationship, please refer to the literature [3–5] and Supplemental Material (SM) [6]. $\tilde{C}_T(k,0)$ has the same dimension as a diffusion constant (in the k space); roughly speaking, random generation of a net flow and its viscous dissipation occur repeatedly, and long-term accumulation of such processes manifests as *diffusion*. In a three-dimensional ordinary liquid, where $\eta(k)$ is nearly constant, the viscous dissipation is accompanied by material flows with $\tilde{C}_T(k,0)/3$ being a (transient) flow-diffusion constant [7]. For the corresponding real-space picture, see SM [6].

In solids, it is known that $\tilde{C}_T(k,\omega)$ at relatively high ω captures the acoustic damping properties and can be described by a simple damped harmonic oscillator model [2], harmonic continuum elasticity with a small viscosity (hereafter, we refer to this as the background viscosity). On the other hand, the properties of $\tilde{C}_T(k,\omega)$ at rather low ω have not been seriously examined thus far. As noting that the viscosity controlling acoustic damping in viscoelastic materials is frequently inconsistent with the terminal ($\omega = 0$) viscosity [8], it is questionable whether the background viscosity can capture the whole aspect of the viscous transport of solid states.

In this study, we reveal a novel transverse viscous dissipation mechanism of solid states, which is different from that determined by the background viscosity, by examining the low ω limit behavior of $\tilde{C}_T(k,\omega)$ and its associated *diffusion* for model solids. We know that significant material diffusion can never occur due to the almost frozen positional degrees of freedom. Contrary to this common belief, we find “transverse diffusion,” but it is different from the usual material diffusion: the corresponding variables are the time integration of the (Eulerian) velocity fields, which are often identified as the true displacement fields, but this is not the case. As demonstrated below, this diffusion is attributed to the existence of a finite terminal viscosity [namely, $\tilde{C}_T(k,0) \neq 0$] specific to solid states. For this purpose, by using soft core potentials [11,12], we perform classical molecular dynamics simulations [13] of

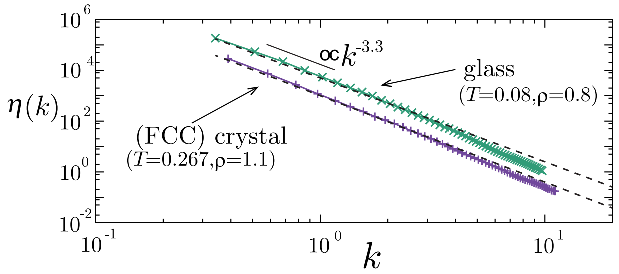

FIG. 1. The k-dependent shear viscosity $\eta(k)$ for the glass and (FCC) crystal states: $\eta(k) \sim k^c$, where the exponent c is close to -3, which agrees with Eq. (13). For the models, see SM [6].

two types of solids: amorphous (glass) and face-centered cubic (FCC) crystalline solids. The details of the simulations and the models are presented in SM [6].

First, in Fig. 1, we show the k-dependent shear viscosity $\eta(k)$ [3–5], which is formally calculated [see Eq. (S5) in SM [6]] for both glass and crystal states, and $\eta(k)$ is found to exhibit a strong k dependence. As mentioned above, a finite value of $\eta(k)$ immediately indicates the existence of some kind of diffusive process. To see what diffuses and to clarify the physical significance, we first investigate the correlation of the following two types of "displacement" fields for a time duration of Δt: (i) one is the displacement field for specific positions of particles defined as

$$\hat{\boldsymbol{u}}_{\boldsymbol{k}}(\Delta t) = \frac{1}{\sqrt{N}} \sum_{j=1}^{N} \int_0^{\Delta t} dt' \boldsymbol{v}_j(t') e^{-i\boldsymbol{k}\cdot\boldsymbol{r}_j^*}, \tag{2}$$

where N is the total number of particles and $\boldsymbol{k}$ is the wave vector. Here, $\boldsymbol{r}_j(t)$ and $\boldsymbol{v}_j(t)$ are the position and velocity of the jth particle at time t, respectively. The corresponding real-space representation is $\hat{\boldsymbol{u}}(\boldsymbol{r}, \Delta t) = \int_0^{\Delta t} dt \hat{\boldsymbol{v}}(\boldsymbol{r}, t)$, with $\hat{\boldsymbol{v}}(\boldsymbol{r}, t) = \sum_{j=1}^N \boldsymbol{v}_j(t)\delta(\boldsymbol{r} - \boldsymbol{r}_j^*)$. Note that the Fourier transform of an arbitrary function $A(\boldsymbol{r})$ is defined by $A_{\boldsymbol{k}} = \int d\boldsymbol{r} e^{-\boldsymbol{k}\cdot\boldsymbol{r}} A(\boldsymbol{r})$. In the following, we set the reference positions $\{\boldsymbol{r}_j^*\}$ for the particle positions at $t = 0$, $\{\boldsymbol{r}_j(0)\}$ [14]. Otherwise, we may use the time-averaged [15] or inherent-state or equilibrium positions as $\{\boldsymbol{r}_j^*\}$ instead of $\{\boldsymbol{r}_j(0)\}$. (ii) The second type of the displacement field may be defined as the time integration of the velocity field:

$$\boldsymbol{u}_{\boldsymbol{k}}(\Delta t) = \frac{1}{\sqrt{N}} \sum_{j=1}^{N} \int_0^{\Delta t} dt \boldsymbol{v}_j(t) e^{-i\boldsymbol{k}\cdot\boldsymbol{r}_j(t)}, \tag{3}$$

whose real-space representation is given by $\boldsymbol{u}(\boldsymbol{r}, \Delta t) = \int_0^{\Delta t} dt \boldsymbol{v}(\boldsymbol{r}, t)$ with $\boldsymbol{v}(\boldsymbol{r}, t) = \sum_{j=1}^N \boldsymbol{v}_j(t)\delta[\boldsymbol{r} - \boldsymbol{r}_j(t)]$ being a microscopic expression of the velocity field [4,5].

These two kinds of displacement fields, Eqs. (2) and (3), are apparently similar to each other, but their transverse parts show completely different behaviors (for the longitudinal components, see SM [6]). In Fig. 2, we show $\langle|\hat{\boldsymbol{u}}_{\boldsymbol{k}}^{\perp}(\Delta t)|^2\rangle$ and $\langle|\boldsymbol{u}_{\boldsymbol{k}}^{\perp}(\Delta t)|^2\rangle$ for various Δt. Hereafter, $[\cdots]^{\perp}$ and $\langle\cdots\rangle$ denote taking the transverse part and an ensemble average, respectively. For $\Delta t \gg t_s$, where t_s is the time for the transverse sound to propagate across the length of the system, $i\boldsymbol{k}\hat{\boldsymbol{u}}_{\boldsymbol{k}}^{\perp} + (i\boldsymbol{k}\hat{\boldsymbol{u}}_{\boldsymbol{k}}^{\perp})^{\dagger}$ can be approximately regarded as a thermally fluctuating elastic shear strain. Therefore, for such Δt [16,17],

$$\langle|\hat{\boldsymbol{u}}_{\boldsymbol{k}}^{\perp}(\Delta t)|^2\rangle \cong \frac{2T}{k^2 G(k)}, \tag{4}$$

where $G(k)$ is the k-dependent shear elastic modulus. For smaller k, $G(k)$ approaches its macroscopic value G, resulting in a k^{-2} dependence of $\langle|\hat{\boldsymbol{u}}_{\boldsymbol{k}}^{\perp}(\Delta t)|^2\rangle$ [14,15,18–21]. On the other hand, $\langle|\boldsymbol{u}_{\boldsymbol{k}}^{\perp}(\Delta t)|^2\rangle$ behaves in a completely different way. Although for smaller Δt and k, $\langle|\boldsymbol{u}_{\boldsymbol{k}}^{\perp}(\Delta t)|^2\rangle$ behaves similarly to $\langle|\hat{\boldsymbol{u}}_{\boldsymbol{k}}^{\perp}(\Delta t)|^2\rangle$, with increasing Δt, the difference between $\langle|\hat{\boldsymbol{u}}_{\boldsymbol{k}}^{\perp}(\Delta t)|^2\rangle$ and $\langle|\boldsymbol{u}_{\boldsymbol{k}}^{\perp}(\Delta t)|^2\rangle$ becomes more pronounced at larger k. $\langle|\boldsymbol{u}_{\boldsymbol{k}}^{\perp}(\Delta t)|^2\rangle$ can be generally related to the VTCF as $\langle|\boldsymbol{u}_{\boldsymbol{k}}^{\perp}(\Delta t)|^2\rangle = \int_0^{\Delta t} ds \int_0^{\Delta t} ds' \langle \boldsymbol{v}_{\boldsymbol{k}}^{\perp}(s) \cdot \boldsymbol{v}_{-\boldsymbol{k}}^{\perp}(s')\rangle$. For a sufficiently large Δt, $(1/3)\int_0^{\Delta t} dt \langle \boldsymbol{v}_{\boldsymbol{k}}^{\perp}(t) \cdot \boldsymbol{v}_{-\boldsymbol{k}}^{\perp}(0)\rangle \cong (1/3)\int_0^{\infty} dt \langle \boldsymbol{v}_{\boldsymbol{k}}^{\perp}(t) \cdot \boldsymbol{v}_{-\boldsymbol{k}}^{\perp}(0)\rangle = \tilde{C}(k, 0)/3$ is the diffusivity of $\boldsymbol{u}_{\boldsymbol{k}}^{\perp}(\Delta t)$, and $\langle|\boldsymbol{u}_{\boldsymbol{k}}^{\perp}(\Delta t)|^2\rangle$ follows [7]

$$\langle|\boldsymbol{u}_{\boldsymbol{k}}^{\perp}(\Delta t)|^2\rangle \cong 2\tilde{C}_T(k, 0)\Delta t \cong \Delta t \frac{4T}{k^2 \eta(k)}, \tag{5}$$

where Eq. (1) is used. Figure 2 shows that Eq. (5) agrees with the simulation results.

This qualitative difference may be surprising because the two definitions $\hat{\boldsymbol{u}}_{\boldsymbol{k}}(\Delta t)$ and $\boldsymbol{u}_{\boldsymbol{k}}(\Delta t)$ have frequently been thought to be physically equivalent as long as particles remain around their reference positions. However, as is

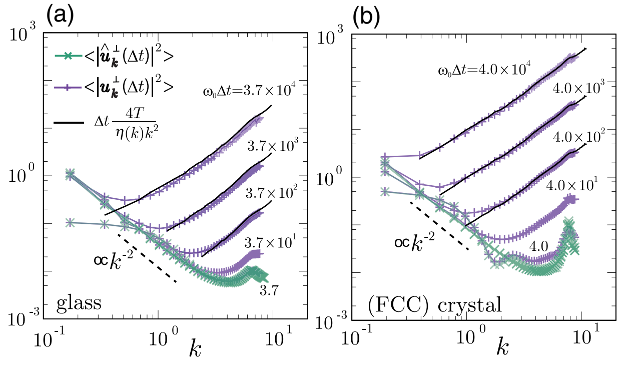

FIG. 2. $\langle|\hat{\boldsymbol{u}}_{\boldsymbol{k}}^{\perp}(\Delta t)|^2\rangle$ and $\langle|\boldsymbol{u}_{\boldsymbol{k}}^{\perp}(\Delta t)|^2\rangle$ for glass (a) and crystal (b) states at various $\Delta t\omega_0$. Here, ω_0 is the average frequency of the thermal vibration of a constituent particle defined as $\omega_0^2 = (1/N)\sum_j 3T/(m_j\langle\delta r_j^2\rangle)$ with m_j and $\langle\delta r_j^2\rangle$ being the mass and the mean square amplitude of the vibration of the jth particle, respectively. Although $\langle|\hat{\boldsymbol{u}}_{\boldsymbol{k}}^{\perp}(\Delta t)|^2\rangle$ collapses on a single line ($\propto k^{-2}$) for $\Delta t\omega_0 \gtrsim 40$, $\langle|\boldsymbol{u}_{\boldsymbol{k}}^{\perp}(\Delta t)|^2\rangle$ grows with Δt. The solid line indicates Eq. (5).

clearly shown in Fig. 2, this is not the case. $\hat{\boldsymbol u}_{\boldsymbol k}(\Delta t)$ represents the collective vibrational fluctuations, while $\boldsymbol u_{\boldsymbol k}(\Delta t)$ undergoes diffusive behavior controlled by $\eta(k)$. In real space, $\hat{\boldsymbol u}(\boldsymbol r, \Delta t)$ represents the displacement measured from the reference positions, but $\boldsymbol u(\boldsymbol r, \Delta t)$ does not [22]. That is, $\boldsymbol u(\boldsymbol r, \Delta t)$ represents a total velocity flow passing the position $\boldsymbol r$ for Δt. The particle positions at which the velocities (momenta) are assigned rapidly fluctuate due to random scattering among the surrounding particles. Such randomness in the positional degrees of freedom is explicitly incorporated into $\boldsymbol v_{\boldsymbol k}(t)$ but not into $\hat{\boldsymbol v}_{\boldsymbol k}(t)$. This random convection in $\boldsymbol v_{\boldsymbol k}(t)$ causes a qualitative difference between $\boldsymbol u_{\boldsymbol k}(t)$ and $\hat{\boldsymbol u}_{\boldsymbol k}(t)$. For solids, one may consider that $\boldsymbol v_{\boldsymbol k}(t)$ follows a damped oscillator model, for which $\tilde{C}_T(k, 0) = 0$ [4], namely, the total passing flow is zero. Contrary to this seemingly reasonable conclusion, the total transverse flow is not zero, and its variance shows a cumulative increase in Δt.

The physical significance of this different behavior between $\boldsymbol u_{\boldsymbol k}(\Delta t)$ and $\hat{\boldsymbol u}_{\boldsymbol k}(\Delta t)$ can be complementarily understood by real-space analysis. For this purpose, we assume a hypothetical cubic box $\mathcal{V}_\ell$ of linear dimension ℓ in a system and define two types of quantities: $\hat{\boldsymbol U}_\ell(\Delta t) = \int_0^{\Delta t} dt' \hat{\boldsymbol V}_\ell(t')$ and $\boldsymbol U_\ell(\Delta t) = \int_0^{\Delta t} dt' \boldsymbol V_\ell(t')$, with $\hat{\boldsymbol V}_\ell(t)$ and $\boldsymbol V_\ell(t)$ being the box-averaged velocities given as

$$\hat{\boldsymbol V}_\ell(t) = \frac{1}{N_\ell(0)} \int_{\mathcal{V}_\ell} d\boldsymbol r \hat{\boldsymbol v}(\boldsymbol r, t) = \frac{1}{N_\ell(0)} \sum_{\{\boldsymbol r_j(0)\} \in \mathcal{V}_\ell} \boldsymbol v_j(t), \tag{6}$$

and

$$\boldsymbol V_\ell(t) = \frac{1}{N_\ell(t)} \int_{\mathcal{V}_\ell} d\boldsymbol r \boldsymbol v(\boldsymbol r, t) = \frac{1}{N_\ell(t)} \sum_{\{\boldsymbol r_j(t)\} \in \mathcal{V}_\ell} \boldsymbol v_j(t), \tag{7}$$

where $N_\ell(t) (\sim \rho \ell^d)$ is the number of particles in the box $\mathcal{V}_\ell$ at time t, ρ is the number density, and d is the spatial dimensionality (here, $d = 3$). $\hat{\boldsymbol U}_\ell(\Delta t)$ is the average displacement of particles assigned to $\mathcal{V}_\ell$ at $t = 0$. On the other hand, similar to $\boldsymbol u(\boldsymbol r, \Delta t)$, $\boldsymbol U_\ell(\Delta t)$ is interpreted as the total flow passing the "box" during the period $[0, \Delta t]$. Accordingly, $\mathcal{V}_\ell$ approximately represents Lagrangian and Eulerian volumes in Eqs. (6) and (7), respectively. In Fig. 3, we plot $\langle |\hat{\boldsymbol U}_\ell(\Delta t)|^2 \rangle$ and $\langle |\boldsymbol U_\ell(\Delta t)|^2 \rangle$ for a glass as a function of ℓ at various Δt. Although the behavior of $\langle |\hat{\boldsymbol U}_\ell(\Delta t)|^2 \rangle \propto \ell^{-1.3}$, which reflects the elasticity [23], remains unchanged, $\langle |\boldsymbol U_\ell(\Delta t)|^2 \rangle$ grows linearly with Δt for smaller ℓ.

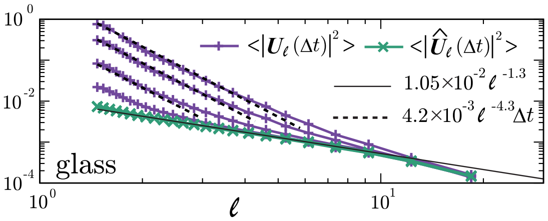

FIG. 3. $\langle |\hat{\boldsymbol U}_\ell(\Delta t)|^2 \rangle$ and $\langle |\boldsymbol U_\ell(\Delta t)|^2 \rangle$ as a function of ℓ in a glass for $\omega_0 \Delta t = 74$, 3.7×10^2, 1.5×10^3, and 3.7×10^4 (see the caption of Fig. 2 for the definition of ω_0). $\langle |\hat{\boldsymbol U}_\ell(\Delta t)|^2 \rangle$ collapses onto a single line ($\propto \ell^{-1.3}$). On the other hand, at smaller ℓ, $\langle |\boldsymbol U_\ell(\Delta t)|^2 \rangle$ linearly grows in Δt.

We emphasize that random ingress and egress of particles (and their momenta) through the box boundaries are explicitly considered only in $\boldsymbol V_\ell(t)$ due to the definition of $\boldsymbol v(\boldsymbol r, t)$. Below, we argue how this effect produces the diffusive behavior of $\boldsymbol U_\ell(\Delta t)$ and is involved in irreversible momentum transfer. Concerning the diffusivity of $\boldsymbol U_\ell(\Delta t)$, the particles, $\{\boldsymbol r_j(t)\} \in \mathcal{V}_\ell$, are categorized into two groups: (A) the particles that are always inside $\mathcal{V}_\ell$ and (B) the particles that randomly vibrate across the box boundaries. Almost recursive trajectories of the (A) particles do not contribute to the diffusive behavior. On the other hand, for the (B) particles, only the trajectories inside $\mathcal{V}_\ell$ are counted, and their random accumulation contributes to the diffusive behaviors of $\boldsymbol U_\ell(\Delta t)$. This situation is schematically shown in Fig. 4. The diffusion coefficient of $\boldsymbol U_\ell(\Delta t)$, D_ℓ, is given as

$$D_\ell \sim \frac{a^3 \omega_0}{\rho \ell^{d+1}}, \tag{8}$$

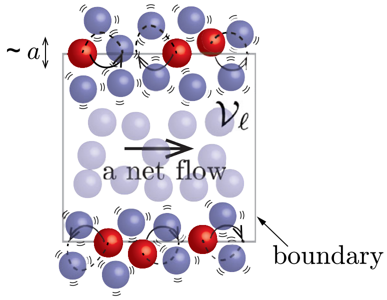

FIG. 4. Schematic of the concept of the diffusive behavior of $\boldsymbol U_\ell(\Delta t)$. ($B$) particles (tagged in red), which randomly vibrate across the boundary of $\mathcal{V}_\ell$, carry their momenta out of $\mathcal{V}_\ell$. They are subsequently scattered by other particles and then return to $\mathcal{V}_\ell$ with different momenta. Such crossing events accompanied by momentum exchanges occur repeatedly with a particle vibration period ($\sim 1/\omega_0$). The crossing direction is somewhat arbitrary due to the randomness in the rotational direction of the particle motion with respect to the reference position [24]. There arises a net flow passing inside $\mathcal{V}_\ell$, and the long-term accumulation of the momentum exchanges manifests as the diffusion of $\boldsymbol U_\ell(\Delta t)$, as shown in Fig. 3. For this behavior, it is essential that the particle velocities and its time integration (trajectories) inside and outside $\mathcal{V}_\ell$ fixed in space are distinguished. This is the case in the *Eulerian* description. If the flows and the trajectories outside $\mathcal{V}_\ell$ (dashed lines) are also considered, diffusive behaviors are absent [also shown for $\hat{\boldsymbol U}_\ell(\Delta t)$ in Fig. 3]. This corresponds to the *Lagrangian* description, in which $\mathcal{V}_\ell$ is supposed to be fixed to matter instead of to space.

where ω_0 and a are the mean frequency and amplitude of the vibration of particles, respectively. A detailed derivation is provided in SM [6]. Equation (8) is consistent with the numerical result for a glass, as shown in Fig. 3(a), for which $a \sim 0.1$ and $\omega_0 \sim 4$ at $T = 0.08$ and $\rho = 0.8$, Eq. (8) gives $D_\ell \sim 10^{-2}\ell^{-4}$ (see the caption of Fig. 2 for ω_0).

Let us consider the relationship between the diffusivity of $\boldsymbol{U}_\ell(\Delta t)$ and the momentum transfer. The diffusion coefficient D_ℓ is expressed in terms of the time integral of the autocorrelation of $\boldsymbol{V}_\ell(t)$ as [7]

$$D_\ell = \frac{1}{3}\int_0^\infty dt \langle \boldsymbol{V}_\ell(t) \cdot \boldsymbol{V}_\ell(0) \rangle. \tag{9}$$

Then, we evaluate D_ℓ using the following conditions. (i) As mentioned above, only the (B) particles contribute to D_ℓ. We accordingly decompose $\boldsymbol{V}_\ell(t)$ into two parts: $\boldsymbol{V}_\ell(t) = \boldsymbol{V}_\ell^{(A)}(t) + \boldsymbol{V}_\ell^{(B)}(t)$. For $\boldsymbol{V}_\ell^{(A)}(t)$ and $\boldsymbol{V}_\ell^{(B)}(t)$, the summation in Eq. (7) is restricted to the (A) and (B) particles, respectively. (ii) As a (B) particle (number j) moves from the inside to the outside of $\mathcal{V}_\ell$, its velocity is transferred to the outer region. Simultaneously, $\boldsymbol{v}_j(t)$ is deleted from $\boldsymbol{V}_\ell(t)$ [and thus from $\boldsymbol{V}_\ell^{(B)}(t)$]. This direct momentum loss occurs for approximately the particle-vibration period ($\sim 1/\omega_0$), resulting in a rapid decay of $\langle \boldsymbol{V}_\ell^{(B)}(t) \cdot \boldsymbol{V}_\ell^{(B)}(0) \rangle$, namely, $\langle \boldsymbol{V}_\ell^{(B)}(1/\omega_0) \cdot \boldsymbol{V}_\ell^{(B)}(0) \rangle \cong 0$. With these two conditions, (i) and (ii), in the integral of Eq. (9) $\langle \boldsymbol{V}_\ell(t) \cdot \boldsymbol{V}_\ell(0) \rangle$ is replaced by $\langle \boldsymbol{V}_\ell^{(B)}(t) \cdot \boldsymbol{V}_\ell^{(B)}(0) \rangle$ with the infinite upper limit being replaced by $1/\omega_0$:

$$D_\ell \cong \frac{1}{3}\int_0^{1/\omega_0} dt \langle \boldsymbol{V}_\ell^{(B)}(t) \cdot \boldsymbol{V}_\ell^{(B)}(0) \rangle \sim \frac{\langle |\boldsymbol{V}_\ell^{(B)}(0)|^2 \rangle}{\omega_0}. \tag{10}$$

Here, $\langle |\boldsymbol{V}_\ell^{(B)}(0)|^2 \rangle$ is evaluated as follows. We set $\boldsymbol{V}_\ell^{(B)}(0) = [1/N_\ell(0)]\sum'_{\{\boldsymbol{r}_j(0)\}\in\mathcal{V}_\ell} \boldsymbol{v}_j(0)$ with the dash denoting that the summation is restricted to the (B) particles. Because they are located around the boundary surface region of width $\sim a$, the number of such particles is approximated as $\rho a \ell^{d-1}$, while $N_\ell \sim \rho \ell^d$. Therefore, $\langle |\boldsymbol{V}_\ell^{(B)}(0)|^2 \rangle = [1/N_\ell(0)^2]\sum'_{\{\boldsymbol{r}_j(0)\}\in\mathcal{V}_\ell} \langle |\boldsymbol{v}_j(0)|^2 \rangle \sim (1/\rho^2\ell^{2d}) \times \rho a \ell^{d-1} \times (T/m) \sim a^3\omega_0^2/(\rho\ell^{d+1})$, where we make use of the equipartition theorem, $\langle \boldsymbol{v}_j(0)\boldsymbol{v}_{j'}(0) \rangle = (3T/m)\delta_{jj'} \sim a^2\omega_0^2\delta_{jj'}$. We subsequently obtain $D_\ell \sim (a^3\omega_0/\rho\ell^{d+1})$, which is consistent with Eq. (8).

Equation (10) is interpreted as a consequence of random momentum exchanges between $\mathcal{V}_\ell$ and the outer region, namely, the repeated occurrence of the random injection and ejection of momenta through the boundaries. As in usual Brownian motion, the consecutive accumulation of such a random momentum exchange results in a "diffusive" motion of $\boldsymbol{U}_\ell$. Notably, this Brownian motion does not apply to the material-element displacement itself. In contrast, for $\hat{\boldsymbol{V}}_\ell(t)$ defined in the Lagrangian volume, the ingress and egress of particles and their momenta are not considered. Thus, the rapid and direct momentum loss through the boundaries is absent; for $\hat{\boldsymbol{V}}_\ell(t)$, the (B) particles for $\boldsymbol{V}_\ell(t)$ are absent. This difference in the definition of the box-averaged velocity causes different behavior between $\langle |\boldsymbol{U}_\ell(\Delta t)|^2 \rangle$ and $\langle |\hat{\boldsymbol{U}}_\ell(\Delta t)|^2 \rangle$.

Such momentum exchanges can be formally described using the friction coefficient or viscosity [7]. The time evolution of the momentum defined in the Eulerian volume by $\boldsymbol{J}_\ell(t) = [1/N_\ell(t)]\sum_{\{\boldsymbol{r}_j(t)\}\in\mathcal{V}_\ell} m_j \boldsymbol{v}_j(t) = [1/N_\ell(t)]\int_{\mathcal{V}_\ell} d\boldsymbol{r}\boldsymbol{j}(\boldsymbol{r}, t)$, where $\boldsymbol{j}(\boldsymbol{r}, t)$ is the momentum field, can be formally expressed in the generalized Langevin equation as

$$\frac{d}{dt}\boldsymbol{J}_\ell(t) = -\int_{-\infty}^{t} dt' \zeta_\ell(t - t')\boldsymbol{J}_\ell(t') + \boldsymbol{\Theta}_\ell(t), \tag{11}$$

where $\zeta_\ell(t)$ is the memory kernel and $\boldsymbol{\Theta}_\ell(t)$ is the noise term. Here, defining the correlation function $H_\ell(t) = \langle \boldsymbol{J}_\ell(t) \cdot \boldsymbol{J}_\ell(0) \rangle$, we obtain $(d/dt)H_\ell(t) = -\int_{-\infty}^{t} dt' \zeta_\ell(t - t')H_\ell(t')$, using the relation $\langle \boldsymbol{\Theta}_\ell(t) \cdot \boldsymbol{J}_\ell(0) \rangle = 0$. In the frequency (ω) space, we obtain

$$\tilde{\zeta}_\ell(\omega) = \frac{-i\omega\tilde{H}_\ell(\omega) + H_\ell(0)}{\tilde{H}_\ell(\omega)}, \tag{12}$$

where $\tilde{\zeta}_\ell(\omega) = \int_0^\infty dt e^{-i\omega t}\zeta_\ell(t)$ and $\tilde{H}_\ell(\omega) = \int_0^\infty dt e^{-i\omega t}H_\ell(t)$. In $\omega \to 0$, Eq. (12) gives $\tilde{\zeta}_\ell(0) = H_\ell(0)/\tilde{H}_\ell(\omega = 0) \sim T/M_\ell D_\ell$, Here, $H_\ell(0) = \langle |\boldsymbol{J}_\ell(0)|^2 \rangle \sim TM_\ell$ from the equipartition theorem and $\tilde{H}_\ell(\omega = 0) = \int_0^\infty dt H_\ell(t) \cong M_\ell^2 \int_0^\infty dt \langle \boldsymbol{V}_\ell(t) \cdot \boldsymbol{V}_\ell(0) \rangle \sim D_\ell M_\ell^2$ from Eq. (9), with M_ℓ being the averaged mass of the box $\mathcal{V}_\ell$. Equation (11) describes the "Brownian" motion of $\boldsymbol{U}_\ell(\Delta t)$, for which $\tilde{\zeta}_\ell(0)M_\ell$ is the friction coefficient of the long-time-scale dynamics. For $d = 3$, by expressing $\tilde{\zeta}_\ell(0)M_\ell$ in terms of Stokes friction as $\tilde{\zeta}_\ell(0)M_\ell \sim \eta_\ell \ell$, we obtain the length-scale-dependent shear viscosity η_ℓ as

$$\eta_\ell \sim \frac{T}{\ell D_\ell} \sim \frac{\rho T}{a^3\omega_0}\ell^3. \tag{13}$$

Note that the corresponding representation of $D_\ell \sim T/(\eta_\ell \ell)$ is $\tilde{C}_T(k, \omega) \cong 2T/[k^2\eta(k)]$, Eq. (1), in the k space. For $k \sim 2\pi/\ell$, the k-dependent shear viscosity $\eta(k)$ is of the form, $\eta(k) \sim \eta_{\ell\sim 2\pi/k} \sim \rho T/a^3\omega_0 k^3$, which is consistent with the numerical results shown in Fig. 1. This length-scale dependence of the viscosity does not originate from structural heterogeneities (e.g., defects or soft spots). In solids, the constituent particles that substantially carry momenta slightly fluctuate around their reference positions. The accompanying small random convection of the velocity in the transverse direction induces irreversible momentum exchanges among neighboring regions. Therefore, we may say that the viscosity studied here is the *renormalized* viscosity accounting for the inertia effect, and is different from the *bare* background viscosity [2,25].

In summary, we have argued a novel transverse viscous transport in solid states that was not previously recognized. In the literature concerning the transverse mechanical and transport properties in solids, the dynamic structure factor $\tilde{S}_T(k,\omega) \cong (\rho_m^2 k^2/\pi\omega^2)\mathrm{Re}\tilde{C}_T(k,\omega)$ is frequently analyzed instead of $\tilde{C}_T(k,\omega)$. Here, ρ_m is the average mass density. In molecular dynamics simulations, $\tilde{S}_T(k,\omega)$ shows three peaks: two symmetric Brillouin peaks and one central peak. The Brillouin peaks can be well captured by a simple damped harmonic oscillator model [2,4] with the background viscosity (see, for example, Refs. [26,27]). Because the main focus of past studies has been placed on acoustic propagation properties, the central peak has received less attention and has been implicitly assumed to be attributable to pure elasticity. However, in our perspective, the central peak should reflect a nontrivial shear viscosity, which is asymptotically expressed as $\tilde{S}_T(k,\omega) = 2\rho_m^2 T/[\pi\omega^2\eta(k)]$.

Before closing, we present the following remarks. The transverse diffusion associated with the terminal viscosity is observed only in the Eulerian description. In the Lagrangian description, there is no diffusive behavior, indicating that $\tilde{C}_T(k,0) = 0$. Because $\eta(k)$ is associated with $\tilde{C}_T(k,0)$ through Eq. (1), $\eta(k)$ should be absent in the Lagrangian description. As the solid dynamics are commonly described in the Lagrangian description instead of in the Eulerian description, one may consider that the viscosity studied here is merely conceptual. However, in supercooled liquids, where the Eulerian description is generally supposed, such viscous transport is also revealed [9,28–31]. Supercooled liquids exhibit both liquidlike and solidlike mechanical properties depending on the timescale [32,33]. At timescales smaller than the structural relaxation time τ_α, a system is regarded as a solid, whereas the viscous response is dominant in the transverse modes for a significant range of k [9]. The resultant terminal viscosity $\eta(k)$ exhibits a marked k dependence similar to those shown in Fig. 1 at mesoscopic length scales [9,28–31]. At larger length scales, $\eta(k)$ approaches the macroscopic viscosity ($\propto \tau_\alpha$), while at microscopic scales, $\eta(k)$ is close to the background viscosity. In the limit of $\tau_\alpha \to \infty$, $\eta(k)$ in liquid states is continuously connected to that in solid states with $\eta(k=0) = \infty$ in the Eulerian description, which is not consistent with the transverse dynamics of solids in the Lagrangian description. In the Lagrangian description, the material displacements measured from the reference positions are the basic observables, while in the Eulerian description, they are the velocities passing arbitrary points. This difference may illuminate different aspects of an identical phenomenon in materials: the viscous response of the *irreversible* momentum flows in the Eulerian description and the elastic response of the *reversible* deformations in the Lagrangian description. They can be translated to each other in principle, but it is almost impossible in general. The present results may pose a fundamental problem for continuum mechanics: how to reconcile liquid and solid descriptions in $\tau_\alpha \to \infty$. We will investigate these issues further elsewhere.

This work was supported by the Japan Society for the Promotion of Science KAKENHI (Grants No. 26103507, No. 25000002, and No. 20H05619) and the special fund of Institute of Industrial Science, The University of Tokyo.

---

[*] furu@iis.u-tokyo.ac.jp

[1] L. D. Landau and E. M. Lifshitz, *Fluid Mechanics* (Pergamon Press, New York, 1959).
[2] L. D. Landau and E. M. Lifshitz, *Theory of Elasticity* (Pergamon Press, New York, 1973).
[3] W. E. Alley and B. J. Alder, Phys. Rev. A **27**, 3158 (1983).
[4] J. P. Boon and S. Yip, *Molecular Hydrodynamics* (Dover, New York, 1991).
[5] J. P. Hansen and I. R. McDonald, *Theory of Simple Liquids* (Academic Press, Oxford, 1986).
[6] See Supplemental Material at http://link.aps.org/supplemental/10.1103/PhysRevLett.127.245901 for additional details of calculations and simulations.
[7] R. Kubo, M. Toda, and N. Hashitsume, *Statistical Physics II, Nonequilibrium Statistical Mechanics* (Springer-Verlag, Berlin, Heidelberg, 1985).
[8] In supercooled liquids, the background viscosity evaluated from $\tilde{C}(k,\omega)$ at higher ω is much smaller than the terminal ($\omega = 0$) viscosity [9]. This is also the case in polymer solutions at mesoscopic length scales (mm $\sim$ μm): The linear hydrodynamic model [10] predicts that the acoustic damping is controlled by the solvent viscosity η_s, which, however, is different from the terminal viscosity, $\eta_p + \eta_s$, with $\eta_p (\gg \eta_s)$ being the polymeric viscosity.
[9] A. Furukawa and H. Tanaka, Phys. Rev. E **84**, 061503 (2011).
[10] A. Furukawa, J. Phys. Soc. Jpn. **72**, 1436 (2003).
[11] B. Bernu, Y. Hiwatari, and J. P. Hansen, J. Phys. C **18**, L371 (1985).
[12] B. Bernu, J. P. Hansen, Y. Hiwatari, and G. Pastore, Phys. Rev. A **36**, 4891 (1987).
[13] D. C. Rapaport, *The Art of Molecular Dynamics Simulation* (Cambridge University Press, Cambridge, 2004).
[14] E. Flenner and G. Szamel, Phys. Rev. Lett. **114**, 025501 (2015).
[15] C. L. Klix, F. Ebert, F. Weysser, M. Fuchs, G. Maret, and P. Keim, Phys. Rev. Lett. **109**, 178301 (2012).
[16] P. M. Chaikin and T. C. Lubensky, *Principles of Condensed Matter Physics* (Cambridge University Press, Cambridge, England, 1995).
[17] Here, the elastic free energy and the shear stress tensor associated with the transverse displacement fluctuations are assumed to be given as $F_{\mathrm{el}} = (1/2)\int_{\boldsymbol{k}}[G(k)|\boldsymbol{k}\hat{\boldsymbol{u}}_{\boldsymbol{k}}^{\perp} + (\boldsymbol{k}\hat{\boldsymbol{u}}_{\boldsymbol{k}}^{\perp})^{\dagger}|^2]$ and $G(k)[i\boldsymbol{k}\hat{\boldsymbol{u}}_{\boldsymbol{k}}^{\perp} + (i\boldsymbol{k}\hat{\boldsymbol{u}}_{\boldsymbol{k}}^{\perp})^{\dagger}]$, respectively.
[18] B. Illing, S. Fritschi, D. Hajnal, C. Klix, P. Keim, and M. Fuchs, Phys. Rev. Lett. **117**, 208002 (2016).

[19] S. Fritschi and M. Fuchs, J. Phys. Condens. Matter **30**, 024003 (2018).

[20] M. Maier, A. Zippelius, and M. Fuchs, J. Chem. Phys. **149**, 084502 (2018).

[21] L. Klochko, J. Baschnagel, J. P. Wittmer, and A. N. Semenov, Soft Matter **14**, 6835 (2018).

[22] Because $\boldsymbol{v}_j(t)e^{-i\boldsymbol{k}\cdot\boldsymbol{r}_j(t)} = [\partial/\partial t + i\boldsymbol{k}\cdot\boldsymbol{v}_j(t)][\boldsymbol{r}_j(t) - \boldsymbol{r}_j(0)]e^{-i\boldsymbol{k}\cdot\boldsymbol{r}_j(t)}$, Eq. (3) does not describe the true displacement.

[23] $\langle|\hat{\boldsymbol{u}}_{\boldsymbol{k}}^{\perp}(\Delta t)|^2\rangle \sim k^{-2}$ indicates r^{-1} correlation in real space, leading to $\langle\hat{\boldsymbol{U}}_{\ell}^2\rangle \sim \ell^{-1}$.

[24] Although the translational motions of the particle are bound, the rotational motions are not: there is an arbitrariness in the rotational directions of the particle motion. That is, the number of times the particle turns around the reference position clockwise or counterclockwise is stochastic, like coin tosses.

[25] The transverse viscous transport studied here is intrinsic to solid systems with the constituents having their reference positions, so it does not depend on whether the considered system is crystalline ordered or amorphous disordered.

[26] H. Shintani and H. Tanaka, Nat. Mater. **7**, 870 (2008).

[27] G. Monaco and S. Mossa, Proc. Natl. Acad. Sci. U.S.A. **106**, 3659 (2009).

[28] J. Kim and T. Keyes, J. Phys. Chem. B **109**, 21445 (2005).

[29] A. Furukawa and H. Tanaka, Phys. Rev. Lett. **103**, 135703 (2009).

[30] R. M. Puscasu, B. D. Todd, P. J. Daivis, and J. S. Hansen, J. Chem. Phys. **133**, 144907 (2010).

[31] A. Furukawa and H. Tanaka, Phys. Rev. E **94**, 052607 (2016).

[32] J. C. Dyre, Rev. Mod. Phys. **78**, 953 (2006).

[33] K. Binder and W. Kob, *Glassy Materials and Disordered Solids* (World Scientific, Singapore, 2005).